doi:10.1016/S0022-2836(02)00388-1 available online at http://www.idealibrary.com on IDEAL® J. Mol. Biol. (2002) 319, 1133–1142

JMB

Mechanism of Coenzyme Recognition and Binding Revealed by Crystal Structure Analysis of Ferredoxin–NADP$^+$ Reductase Complexed with NADP$^+$

Juan A. Hermoso[1]*, Tomas Mayoral[1], Merche Faro[2] Carlos Gómez-Moreno[2], Julia Sanz-Aparicio[1] and Milagros Medina[2]

[1]*Grupo de Cristalografía Macromolecular y Biología Estructural, Instituto Química-Física Rocasolano C.S.I.C., Serrano 119, 28006 Madrid, Spain*

[2]*Departamento de Bioquímica y Biología Molecular y Celular Facultad de Ciencias Universidad de Zaragoza 50009 Zaragoza, Spain*

**Corresponding author*

The flavoenzyme ferredoxin–NADP$^+$ reductase (FNR) catalyses the production of NADPH in photosynthesis. The three-dimensional structure of FNR presents two distinct domains, one for binding of the FAD prosthetic group and the other for NADP$^+$ binding. In spite of extensive experiments and different crystallographic approaches, many aspects about how the NADP$^+$ substrate binds to FNR and how the hydride ion is transferred from FAD to NADP$^+$ remain unclear. The structure of an FNR:NADP$^+$ complex from *Anabaena* has been determined by X-ray diffraction analysis of the cocrystallised units to 2.1 Å resolution. Structural perturbation of FNR induced by complex formation produces a narrower cavity in which the 2′-phospho-AMP and pyrophosphate portions of the NADP$^+$ are perfectly bound. In addition, the nicotinamide mononucleotide moiety is placed in a new pocket created near the FAD cofactor with the ribose being in a tight conformation. The crystal structure of this FNR:NADP$^+$ complex obtained by cocrystallisation displays NADP$^+$ in an unusual conformation and can be considered as an intermediate state in the process of coenzyme recognition and binding. Structural analysis and comparison with previously reported complexes allow us to postulate a mechanism which would permit efficient hydride transfer to occur. Besides, this structure gives new insights into the postulated formation of the ferredoxin:FNR:NADP$^+$ ternary complex by prediction of new intermolecular interactions, which could only exist after FNR:NADP$^+$ complex formation. Finally, structural comparison with the members of the broad FNR structural family also provides an explanation for the high specificity exhibited by FNR for NADP$^+$/H *versus* NAD$^+$/H.

Keywords: ferredoxin–NADP$^+$ reductase; coenzyme binding; NADPH; NADH; X-ray structure

Introduction

Although the general mechanism of action for many flavoenzymes is known, the mechanism of the hydride ion transfer between the isoalloxazine ring and the nicotinamide ring of the coenzyme is not completely understood for most of them. This is the case for ferredoxin–NADP$^+$ reductase (FNR) and other structurally related enzymes. Three-dimensional structures of FNR from different sources have been determined in their oxidised[1–4] and reduced states.[2] FNR consists of two distinct domains, one responsible for binding of the FAD prosthetic group and the other for NADP$^+$ binding. This unique structural two-domain motif has been proposed to be a prototype for a large family of flavoproteins.[5] Structurally characterised members of this family involve phthalate dioxygenase reductase[6] (PDR), the FAD-containing fragment of the NADH-dependent nitrate reductase,[7] cytochrome b_5 reductase,[8] NADPH-cytochrome P450 reductase,[9] flavodoxin reductase[10] and sulfite reductase.[11]

Abbreviations used: FNR, ferredoxin–NADP$^+$ reductase; Fd, ferredoxin; NMN, nicotinamide monoucleotide portion of NADP$^+$/H; 2′P-AMP, 2′-phospho-AMP portion of NADP$^+$/H; βOG, β-octylglucoside; PEG, polyethylene glycol; PDR, phthalate dioxygenase reductase.

E-mail address of the corresponding author: xjuan@iqfr.csic.es

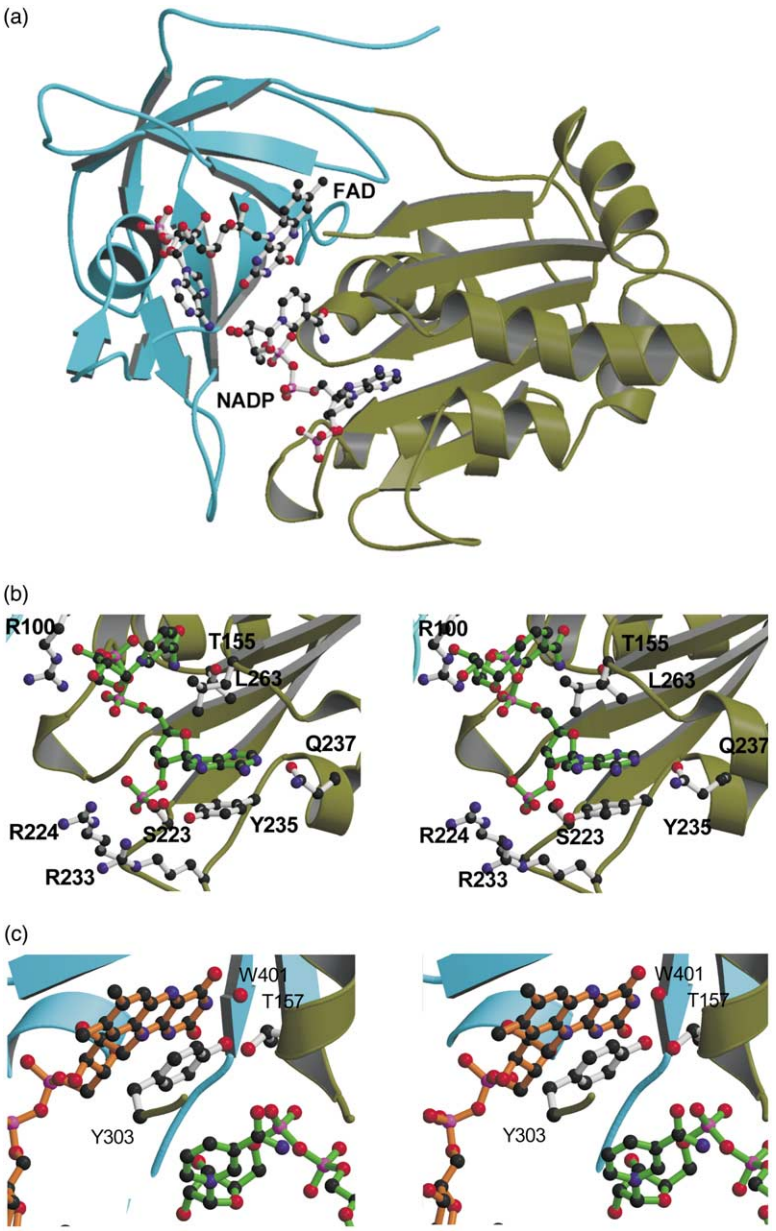

Figure 1. Overall structure of the FNR:NADP$^+$ complex and enzyme–coenzyme interactions. (a) Ribbon diagram of the FNR:NADP$^+$ complex, with the FAD prosthetic group and NADP$^+$ coenzyme represented as balls and sticks, and the protein-binding domains for each cofactor being coloured in cyan and green, respectively. (b) FNR residues interacting with NADP$^+$ (coloured in green) are represented as ball and sticks. (c) Relative positions of isoalloxazine (orange) and nicotinamide (green) rings in the FNR:NADP$^+$ complex. In spite of the proximity between both rings there is no displacement of Tyr303. This C-terminal Tyr is well stabilised by a stacking interaction with the isoalloxazine ring and by a bifurcated hydrogen bond with a water molecule and Thr157.

In plants, algae and cyanobacteria FNR plays a strategic role during photosynthesis by mediating the reversible two-electron transfer between two molecules of the one-electron carrier ferredoxin (Fd) and a single NADP$^+$/H molecule.[12] It is proposed that this process requires the formation of a transient ternary complex between the three partners, FNR, NADP$^+$ and Fd, in which oxidised FNR is thought to form a complex with NADP$^+$ prior to its association with reduced Fd.[13] Once the FNR is fully reduced, the flavin and the nicotinamide rings must be placed in a relative orientation such that functional hydride transfer from N5 of the flavin to C4 of the nicotinamide would be allowed. These conditions could be only achieved by disruption of the stacking interaction of the FNR C-terminal Tyr side-chain with the isoalloxazine ring or by changes in the relative orientation of the two protein domains in the FNR. Only a few structures of flavoenzymes bound to NADP$^+$ in a "productive" mode are available. In the case of glutathione reductase and NADPH peroxidase the nicotinamide and flavin ring planes are parallel, making extensive contacts, and the C4 of the nicotinamide is just 3.8 Å of N5 from the flavin.[14–16] In NAD(P)H–quinone reductase, however, although both rings are also parallel there is no superposition of the central part of the flavin with the nicotinamide ring.[17] The crystal structure of a ferric reductase in complex with NADP$^+$ also shows a packing of the NMN (nicotinamide mononucleotide) half of the coenzyme and the isoalloxazine ring.[18] However, this enzyme differs significantly from FNR, since it possesses neither an NADP$^+$-binding domain able to discriminate between NADP$^+$/H and NAD$^+$/H, nor an aromatic residue packing against the flavin ring in the position where the

nicotinamide is expected to bind. Complexes with $NADP^+$/H of FNR forms from different species have always resulted in a nicotinamide ring either not visible or away from the isoalloxazine ring.[1–3] Only partial success has been reported with a couple of mutants in the pea enzyme, where the terminal Tyr residue was replaced either by Ser or Trp.[19] In these complexes, specially in the Y308S mutant, the obtained structures of the complexes with NADPH and $NADP^+$ are proposed to resemble that of the productive state of the complex. In order to provide a structural guideline for elucidating the mechanism of electron transfer from FNR to the coenzyme we have further studied the interaction between the unmodified enzyme and $NADP^+$ by X-ray crystallography.

Results and Discussion

Structure of the FNR:$NADP^+$ complex

Cocrystallisation of FNR with $NADP^+$ produced crystals with a completely different packing from those of native, wild-type and any mutant so far reported. The structure was solved by molecular replacement, and the electron density maps clearly showed strong density for the complete $NADP^+$ molecule. The crystal structure of this FNR:$NADP^+$ complex has been refined up to 2.1 Å resolution. The overall FNR folding is equivalent to that of the free *Anabaena* FNR. Differences observed in the 104–114 loop seem to be related to the structural flexibility of this region[3,20,21] that it is involved in crystal packing contacts. No significant changes in the relative orientation of the FAD and $NADP^+$-binding domains were observed, and the $NADP^+$ molecule is perfectly complementary within a cavity situated at the C-terminal edge of the parallel β-sheets of the $NADP^+$-binding domain, which extends towards the FAD-binding domain interface (Figure 1(a)). The coenzyme shows a characteristic L-shape with the pyrophosphate group located at the corner and the two branches of the L accommodating the NMN moiety and the 2′-P-AMP, respectively. The adenine moiety of the $NADP^+$ is sandwiched between the hydrophobic Leu263 side-chain and the aromatic ring of Tyr235, and is also making a hydrogen bond with the Gln237 side-chain (Figure 1(b)). The 2′-P group of $NADP^+$ is stabilised by several H-bonds with the side-chains of Ser223, Arg224 and Arg233, and the OH group of Tyr235. Two H-bonds are also detected between 2′-P and residues Lys105 and Thr112 of a symmetry-related FNR molecule. The pyrophosphate moiety of $NADP^+$ is essentially stabilised by the guanidinium group of Arg100. The nicotinamide moiety is only stabilised by two polar interactions with Thr155 and by a van der Waals contact with Leu263. It is worth noting the very tight conformation in which the ribose is found, specially considering that no interactions with the enzyme are found which could account for this feature. This may be related to the enzymatic mechanism as will be discussed below.

Finally, Tyr303 is stacked between the isoalloxazine and the nicotinamide rings with the NADP C4 atom being 7.78 Å far from the FAD N5 atom (Figure 1(c)). Besides, nicotinamide ring presents its B-face to the Re-face of the FAD and therefore is not orientated properly according to the stereospecificity defined for FNR. Therefore, it is remarkable that although in this complex the nicotinamide ring of the $NADP^+$ is placed near the isoalloxazine ring, it does not replace the C-terminal Tyr as it has been proposed to be required for efficient electron transfer. A similar situation of the nicotinamide moiety has been also observed in a PDR complex with NADH[6] where the nicotinamide is sandwiched between Pro201 and Phe225 in a pocket formed by the pyrophosphate binding segment, a helical turn and the aromatic ring of Phe225.[6] The authors suggest that the structural changes necessary to stack the nicotinamide over the flavin ring require some displacement of the protein backbone as well as movement of the side-chain of the Phe225.

Structural differences between free FNR and the FNR:$NADP^+$ complex

In spite of the good correlation between $NADP^+$-complexed and free FNR forms for the backbone, rearrangements of the regions involving residues 221–239 (C^α rmsd of 0.30 Å) and 261–298 (C^α rmsd of 0.52 Å) are observed upon $NADP^+$ binding (Figure 2(a)). The first region contains the long loop formed by residues 221–235, and the beginning of a small α-helix (236–243), which moves towards the adenine ring and the 2′-P of the coenzyme. With regard to the second region, a less extended conformation of the loop 261–265 as well as a displacement of α-helices D (residues 266–281) and E (residues 285–295) are observed. A small displacement of the adenine moiety of the FAD is also observed. These backbone displacements are also associated with significant changes in conformers for some residues (Figure 2(b)). Thus, a more extended conformer is observed for Arg100, which allows its guanidinium group to stabilise the pyrophosphate group of the coenzyme while, at the same time, provides the necessary space to accommodate the ribose from the NMN moiety of $NADP^+$. Displacement of the 221–239 backbone region is associated with new conformers for Ser223, Arg224, Arg233, Tyr235 and Gln237. Arginine and serine side-chains move towards the coenzyme in order to stabilise its 2′-P (Figure 2(b)). A change in the $\chi 1$ torsion angle of Tyr235 is also observed allowing both, a stacking interaction with the adenine ring, and a polar interaction with the 2′-P. In contrast with the free FNR structure, an ordered conformation for Gln237 side-chain is observed as a consequence of an H-bond with the adenine. With regard to the 261–298 region, the most important change is that

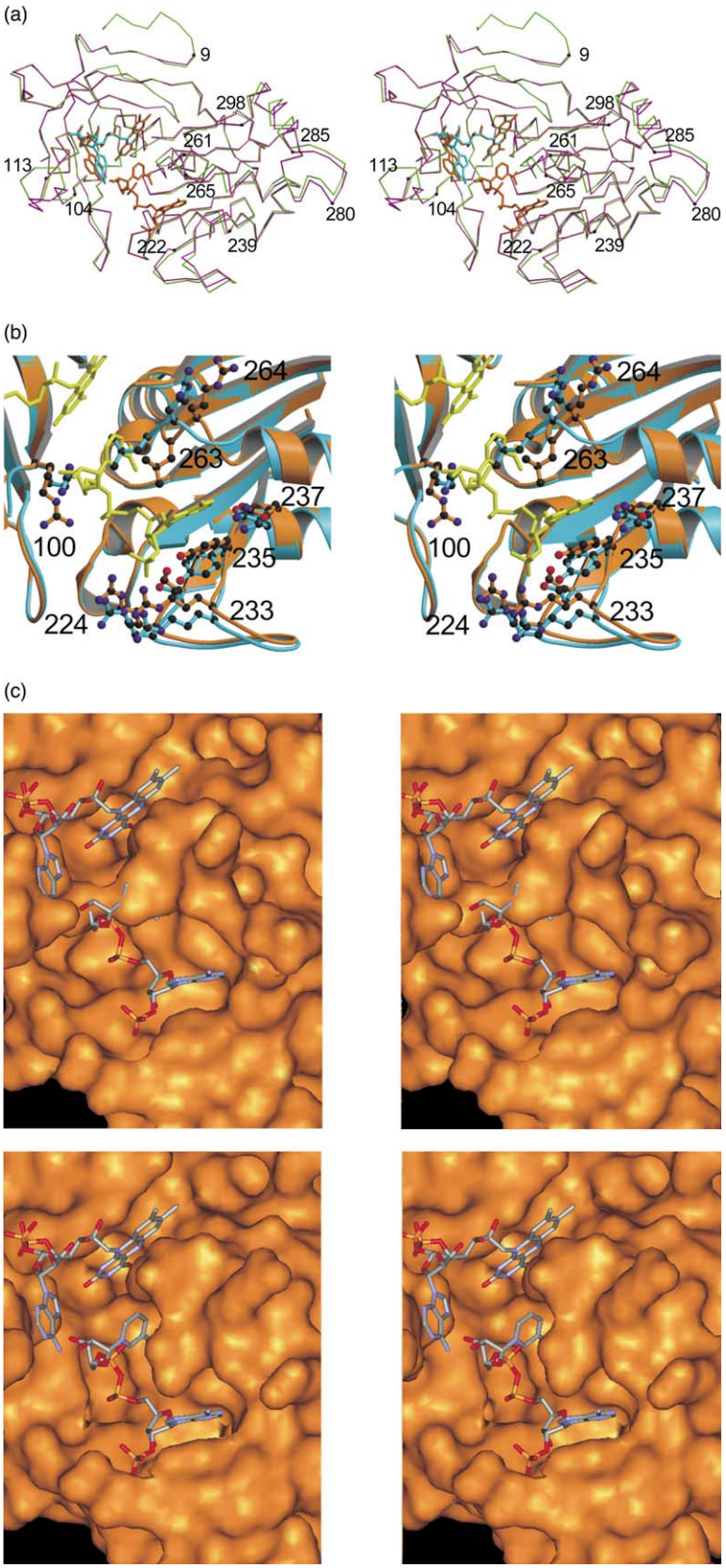

Figure 2. Structural reorganisation of FNR induced by complex formation with $NADP^+$. (a) Stereoview of the free (green) and $NADP^+$-bound enzyme (magenta), superimposed by the least square fitting of the whole FNR. FAD and $NADP^+$ in the complex are coloured in orange, while in the free enzyme FAD is coloured in blue. Regions with significant changes are labelled (b). Residues exhibiting significant changes in conformation upon coenzyme binding are represented as ball and sticks and coloured in blue for free FNR and in orange for FNR:$NADP^+$ complex. (c) Stereoviews of the active site in free enzyme (upper) and FNR:$NADP^+$ complex (lower). $NADP^+$ molecule is also positioned in free FNR for comparison purposes. A narrowing of the cavity in which 2′-P-AMP and pyrophosphate are located is observed upon complex formation.

shown by Leu263 side-chain which moves 3.7 Å from its position in the wild-type enzyme. Such movement allows the nicotinamide ring to be placed in the previous Leu263 position and, most importantly, to simultaneously interact with both the adenine and the nicotinamide rings (Figure 2(b)). Therefore, Leu263 seems to be essential to stabilise the conformation of $NADP^+$ as shown in

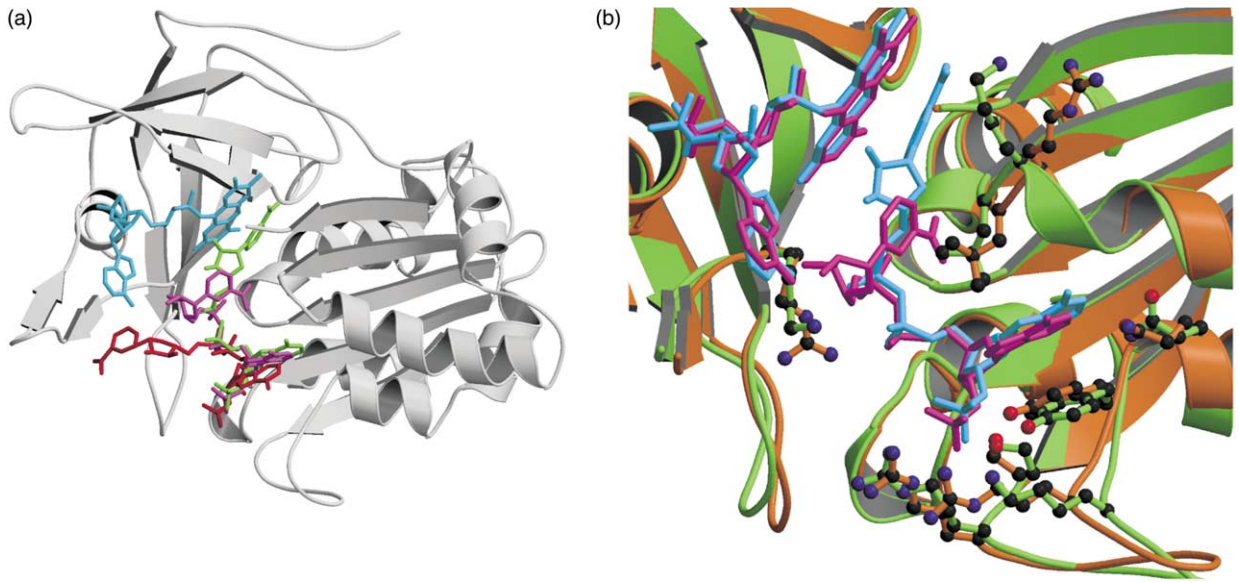

Figure 3. Different $NADP^+$ conformations in the FNR:$NADP^+$ complexes. (a) Superposition of the two $NADP^+$ conformations observed for the different complexes onto the cocrystallised *Anabaena* FNR:$NADP^+$ structure. Coenzyme conformation obtained by soaking[3] is coloured in red (complex I), cocrystallised coenzyme is coloured in magenta (complex II) and $NADP^+$ conformation obtained after mutation of the C-terminal Tyr in pea FNR[19] is coloured in green (complex III). The FAD cofactor is coloured in blue. (b) Superposition of the cocrystallised *Anabaena* FNR:$NADP^+$ complex (orange) and the pea FNR:$NADP^+$ complex (green). FAD and $NADP^+$ cofactors are coloured in magenta for complex II and in cyan for complex III. Residues interacting with $NADP^+$ in both structures are represented as ball and sticks (see Figure 1(b) for labelling).

this complex. Thus, the combined effects described for backbone and side-chains movements produce a narrower cavity in which the 2′-P-AMP and the pyrophosphate moieties are bound in such a way that a perfect complementarity between this coenzyme moiety and the protein surface is produced (Figure 2(c)).

Comparison of different FNR:$NADP^+$ complexes

Three-dimensional structures for FNR:$NADP^+$ complexes have been previously reported for the *Anabaena* and pea enzymes.[3,19] In the case of the previous *Anabaena* FNR:$NADP^+$ complex (complex I), which was obtained by soaking native FNR crystals in an $NADP^+$ solution, no changes were detected in the protein backbone with regard to the free enzyme, and only slight rotations were observed for the side-chain of some residues in order to approximate to the 2′-P group.[3] Complex I only provided reliable binding information for the 2′-P-AMP coenzyme moiety, since the nicotinamide appears pointing towards the molecular surface far away from the FAD isoalloxazine ring (Figure 3(a)). Thus, conformation of $NADP^+$ in the complex I exhibited a more extended conformation than that of the complex presented here (complex II). These changes have to be interpreted in light of the different crystallisation methods used, suggesting that cocrystallisation allows the adaptation between the FNR enzyme and the coenzyme without any kind of steric impediment introduced by the preformed native crystal packing.

The three-dimensional structure of a complex between $NADP^+$ and a pea FNR mutant in which the C-terminal Tyr residue has been replaced by Ser and Trp, has also been reported[19] (complex III). In this complex, $NADP^+$ presents a different conformation from those described for complex I and complex II (Figure 3(a)). Thus, in complex III the pyrophosphate and 2′-P-AMP portions of $NADP^+$ present a similar conformation to the analogous moieties of the complex II and induce equivalent structural rearrangements in the protein to stabilise them. Therefore, similar interactions of $NADP^+$ with residues of regions 261–265 and 221–239 of the FNR are observed in pea complex (Figure 3(b)). However, in complex III removal of the terminal Tyr produces a different configuration of the NMN moiety and a more extended conformation for the ribose. This conformation approaches the nicotinamide group to the FAD isoalloxazine ring and situates its C4 atom at only 3 Å from the N5 atom of the isoalloxazine ring allowing direct hydride transfer.

Insights into the mechanism of molecular recognition and complex reorganisation for hydride transfer between FNR and $NADP^+$

Although the existing structural data show three different binding modes for the $NADP^+$–FNR interaction, none of them represents a functional model for the *in vivo* hydride transfer process. Thus, while in complexes I and II the relative distance between the nicotinamide and the

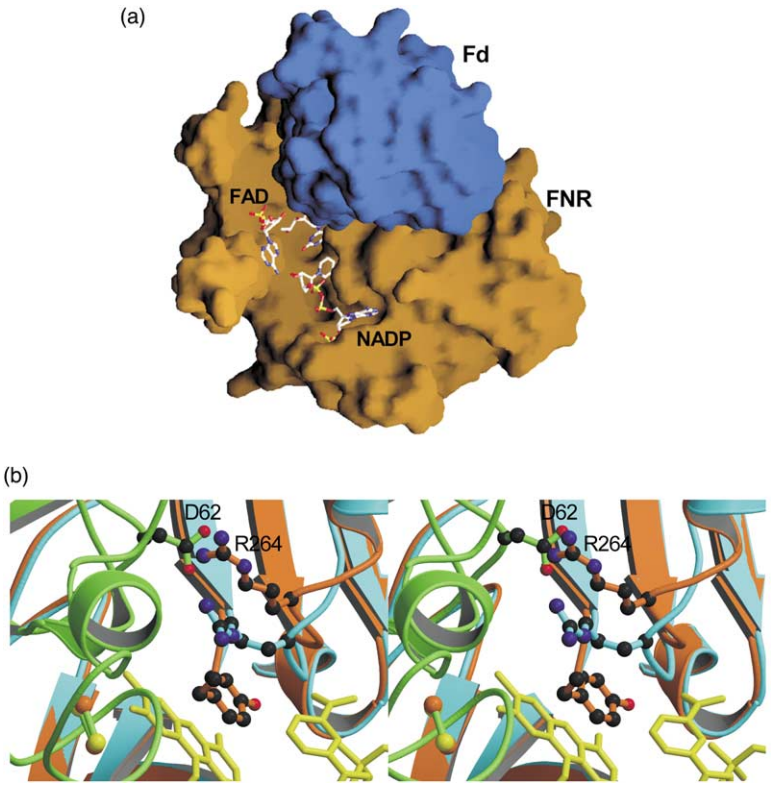

Figure 4. Putative model for a transient Fd:FNR:NADP$^+$ ternary complex in *Anabaena*. This model was obtained by superposition of the FNR coordinates in the Fd:FNR complex[24] with those in the FNR:NADP$^+$ complex. (a) Molecular surface of Fd (blue) and FNR (orange) with FAD and NADP$^+$ cofactors in sticks. (b) New interactions could take place between Fd and FNR after FNR:NADP$^+$ complex formation. Rearrangements in 261–265 loop as observed in complex II (orange) would form a new ion pair between R264 and D62 of Fd (green). In the reported Fd:FNR complex,[24] FNR R264 residue (blue) is far from the Fd D62 residue.

isoalloxazine rings is not adequate to allow the hydride transfer, the complex III can only be obtained upon removal of the terminal Tyr residue. However, this residue has also been proposed to be involved in the catalytic mechanism by modulating pyridine nucleotide affinity.[19,22] Nevertheless, none of these structures excludes the others and can be interpreted as different steps in molecular recognition and complex reorganisation to provide the adequate orientation for the hydride transfer. Thus, complex I might reflect the initial recognition of NADP$^+$ as an FNR coenzyme, through its 2′-P-AMP moiety and the 221–239 region of the protein. The final coenzyme recognition is attained when complex II is produced. Structural rearrangements in this second step are observed in the protein chain in order to better stabilise the 2′-P-AMP and the nicotinamide moieties. The regions involved are the segments 221–239 and 261–298. Besides, a change in the conformation of Arg100 is essential to H-bond the NADP$^+$ pyrophosphate bridge. These protein structural changes are also associated with a change in the NADP$^+$ molecule conformation, which goes from the extended conformation observed in complex I to the more tighten state observed in complex II. Finally, Tyr displacement would allow the nicotinamide ring to approach the isoalloxazine presenting the A-face of the NADP$^+$ to the Re-face of the FAD, as has been observed in complex III. (Figure 3(b)). Moreover, the movement of this Tyr must be essential for catalysis, since it has been shown that it down-modulates the strong affinity of the proposed binding pocket shown in complex III for the NADP$^+$ nicotinamide.[19]

Thus, the key point in this mechanism is how does the terminal Tyr get removed from its stacking position with the flavin ring. The influence of Fd in this event has been investigated by modelling studies.[4] However, the driving force for such displacement still remains unknown, although the biochemical and structural information available permits some hypothesis to be made. First of all, aromatic stacking interactions between activated rings seem to be destabilising as deduced from the model of $\pi-\pi$ interactions proposed by Hunter & Sanders.[23] Therefore, the stacking interaction between Tyr and isoalloxazine rings may even be hindered upon FAD reduction. It is also worth noting that Tyr303 is involved in a bifurcated H-bond with Thr157 and a buried water molecule that is highly conserved in all reported FNR structures (Figure 1(c)). This water has been proposed as an alternative possible proton donor of Ser80 to the isoalloxazine upon reduction.[2] As a consequence, the proton transfer process might weaken the Tyr303–water link and promote movement of Tyr303 towards Thr157. In addition, this movement (downwards in Figure 1(c)) is the only possible way out for the Tyr303 side-chain, since FNR residues prevent movement in the opposite direction. Moreover, the analysis of spectral perturbations upon NADP$^+$ binding to oxidised FNR shows that the nicotinamide ring is not able to alter the absorption spectrum of the flavin ring of cyanobacterial FNRs (including the *Anabaena* one),

suggesting a weak interaction of the nicotinamide with its "putative" binding site for hydride transfer of these enzymes in their oxidised state.[24–26] On the contrary, the spectrum of FNRs from higher plants result clearly modified under the same conditions, pointing to an interaction between the nicotinamide and the flavin group, which suggest some differences in this mechanism among higher plants and cyanobacterial FNRs.[22,24–26] Therefore, all these pieces of structural and biochemical information support the hypothesis that, at least in the case of the *Anabaena* FNR, the Tyr303 displacement could be a direct consequence of both the isoalloxazine reduction and the proton transfer process.

Insights into the Fd:FNR:NADP$^+$ ternary complex and the electron transfer process

Fast kinetic studies suggested that the FNR catalysed electron transfer from Fd to NADP$^+$ proceeds through the formation of a transient ternary complex.[12,13] Thus, the binding of the proteins appears to be ordered for efficient electron transfer, with Fd binding to a preformed FNR:NADP$^+$ complex.[12] Recently, the crystal structure of an *Anabaena* Fd:FNR complex has also been reported,[27] which showed no significant structural modifications in FNR upon Fd binding. The molecular interface between Fd and FNR is formed by a hydrophobic core, a net of 11 hydrogen bonds and one ion pair.[27] On the basis of this structure and that of the complex here presented, we have modelled a putative Fd:FNR:NADP$^+$ ternary complex (Figure 4). This model shows that the NADP$^+$ binding site on FNR is not close to the Fd:FNR interface (Figure 4(a)) and, therefore, previous NADP$^+$ binding to FNR should not affect the interaction between the two proteins. However, upon NADP$^+$ binding, structural rearrangements in the 261–265 loop of FNR are observed that involve changes in the conformation and orientation of Arg264, residue that has been shown to be involved in productive FNR:Fd interaction for electron transfer,[28] which moves in such a way that a putative new ion pair could be formed between its side-chain and that of Asp62 from Fd (Figure 4(b)). This new link would be form through a Fd loop, that has been shown to contain critical residues for FNR binding (like Phe65) and also to be involved in triggering Fd_{ox} release upon electron transfer to FNR.[27,29] Therefore, in the preformed FNR:NADP$^+$ complex such a link between Arg264 FNR and Asp62 Fd could provide a larger affinity for reduced Fd than that exhibited by the free enzyme. Moreover, since a displacement of the loop containing Asp62 in Fd upon reoxidation has been related to the different affinity of FNR for reduced and oxidised ferredoxin,[27] such interaction might also being involved in oxidised Fd releasing. Further biochemical work should be done in order to clarify this point.

Why is FNR an NADP$^+$ specific enzyme?

Recent studies on *Anabaena* FNR indicate that the determinants of the high specificity shown by this enzyme for NADP$^+$/H *versus* NAD$^+$/H is not only provided by those residues directly interacting with the 2′-P, despite the fact that this is the only difference between the two coenzymes.[25,30] Moreover, these studies also pointed to other regions of the protein that, although not interacting directly with the coenzyme, must undergo specific structural arrangements of the backbone chain in order to determine coenzyme specificity. Sequence and structure analysis of different members of the FNR family with affinity for either NADP$^+$/H or NAD$^+$/H, suggested that the region formed by residues 155–161 of *Anabaena* FNR might be involved in such discrimination. Biochemical and structural characterisation of an *Anabaena* FNR mutant in which, Thr155, (a residue conserved in all NADP$^+$/H-dependent members of the family) had been replaced by Gly (a residue present in all NAD$^+$/H-dependent members) has been reported.[25] It was observed that this replacement produced an important modification of the FNR 261–265 loop. The equivalent region in the NAD$^+$/H-dependent enzymes is rich in proline residues and therefore quite rigid.

Superposition of the NADP$^+$ binding domain of the FNR:NADP$^+$ complex presented here with the corresponding domain of several NAD$^+$/H-dependent members of the FNR family (phthalate dioxygenase reductase, PDB code 2PIA, cytochrome b_5 reductase, code 2CND and the NADH-dependent nitrate reductase, code 1NDH) shows a closer conformation for the 261–265 loop (see Figure 2) than that obtained when comparing with the free FNR. In particular, a proline residue of the above mentioned Pro-rich loop in the NAD$^+$/H-dependent enzymes is systematically placed at the same position that the critical Leu263 residue of the FNR:NADP$^+$ complex. These observations clearly suggest different mechanisms for coenzyme recognition and complex reorganisation in FNR, and therefore in NADP$^+$/H-dependent members of the FNR family relative to the NAD$^+$/H-dependent members. Thus, in the case of the FNR, it seems that the free enzyme presents a large cavity to accommodate the 2′-P-AMP moiety of the coenzyme, which upon its binding is reorganised in order to match perfectly the charge and shape of the adenine portion of the substrate. However, in the case of the NAD$^+$/H-dependent members, such a narrow cavity is already preformed in the free enzyme and probably does not need to undergo important structural rearrangements in order to adapt the adenine moiety of NAD$^+$/H as it has been described in the case of PDR:NADH complex.[6] In summary, the coenzyme specificity in the FNR family can be explained as a consequence of the nature of both, the residues interacting directly with the 2′P phosphate and the residues shaping the pocket that accommodates the AMP.

Table 1. Structure determination statistics

Crystal data	
Space group	($I4_1$)
a (Å)	151.69
b (Å)	151.69
c (Å)	35.44
Data collection[a]	
Wavelength (Å)	1.5418
Resolution (Å)	2.1 (2.21–2.1)
Unique data	23,930
Redundancy	3.8 (3.8)
Completeness (%)	99.5 (99.5)
$I/\sigma(I)$	4.4 (1.9)
R_{sym} (%)[b]	0.10 (0.38)
Refinement	
Resolution range (Å)	29.7–2.1
R_{work} (R_{free})[c]	0.20 (0.27)
Rmsd[d] bonds (Å)	0.011
Rmsd angles (°)	1.239
Quality of Ramachandran plot[e]	
Percentage of residues in most favoured regions	89.1
Percentage of residues in additional allowed regions	10.9
Percentage of residues in generously allowed regions	0.0
Number of atoms (*average* B-*values* (Å^2))	
Protein	2334 (32.5)
Water	200 (39.7)
$NADP^+$	48 (35.8)

[a] Values in parentheses correspond to the highest resolution shell.
[b] $R_{sym} = \sum|I - I_{av}|/\sum I$, where the summation is over symmetry equivalent reflections.
[c] *R* calculated on 7% of data excluded from refinement.
[d] Root-mean-square deviation.
[e] Figures from PROCHECK.

Nevertheless, further mutagenesis studies on the FNR family will clarify the subtle structural features that confer coenzyme specificity.

Conclusions

In the photosynthetic electron transfer chain involved in converting the energy of the light into chemical power, under the form of NADPH reducing equivalents, FNR catalyses the flavin-mediated two-electron transfer from two ferredoxin molecules to $NADP^+$. The FNR structure, formed by two domains, one for binding the FAD and the other for binding $NADP^+$, has provided a structural prototype for a large family of flavoenzymes.

Here, we present the crystal structure of an FNR:$NADP^+$ complex from *Anabaena* that has been obtained by cocrystallisation. This structure differs from those previously reported for FNR:$NADP^+$ complexes in *Anabaena* and pea enzymes, the main difference being the relative position of the $NADP^+$ nicotinamide ring within the complex. However, these different $NADP^+$ conformations do not exclude each other, and together reveal new insights into the catalytic mechanism of FNR, suggesting a model for coenzyme recognition and complex reorganisation for an efficient hydride transfer to occur. Finally, structural comparison between the FNR family provides an explanation for the high specificity exhibited by FNR for $NADP^+$/H *versus* NAD^+/H that could be extended to the rest of members of this family.

Materials and Methods

Expression and purification of FNR

Recombinant FNR was purified from IPTG-induced *Escherichia coli* LB cultures containing the corresponding construct of the *Anabaena pet* H gene as previously described.[25]

Crystallisation and data collection

The FNR:$NADP^+$ crystals were grown by cocrystallisation using the hanging drop method. The 5 μl droplets consisted of 1 μl of 27 mg protein/ml solution buffered with 10 mM Tris/HCl (pH 8.0), 1 μl of 10 mM $NADP^+$, 1 μl of unbuffered βOG at 5% (w/v) and 2 μl of reservoir solution containing 20% (w/v) PEG6000 and 0.1 M sodium acetate (pH 5.0). The droplet was equilibrated against 1 ml reservoir solution at 20 °C. Under these conditions crystals grew within 1–15 days as small needles and only very few experiments led to prisms that increased the maximum size to 0.8 mm × 0.3 mm × 0.2 mm, suitable for X-ray diffraction.

X-ray data for these crystals were collected at 100 K on a Mar Research 345 (Germany) IP area detector using graphite-monochromated CuKα radiation generated by an Enraf–Nonius rotating anode generator. Crystals belong to the $I4_1$ tetragonal space group ($a = b =$ 151.69 Å and c = 35.44 Å). The V_M is 3.0 Å^3 Da^{-1} with one FNR molecule in the asymmetric unit and 59% solvent content. The X-ray data set was processed with MOSFLM[31] and scaled and reduced with SCALA from the CCP4[32] up to 2.1 Å resolution (Table 1).

Structure determination and refinement

The FNR:$NADP^+$ structure was solved by molecular replacement using the program AMoRe[33] on the basis of the 1.8 Å resolution native FNR model.[3] An unambiguous single solution for the rotation and translation functions was obtained. The model was subjected to alternate cycles of conjugate gradient refinement with the program X-PLOR[34] and manual model building with the software package O.[35] The crystallographic *R* of an R_{free}[36] values converged to values of 0.20 and 0.27, respectively, for reflections between 30 Å and 2.1 Å resolution. The resulting electron density was of great quality as can be seen for the case of the $NADP^+$ molecule (Figure 5). The final model contains 2334 non-hydrogen protein atoms, one $NADP^+$, one FAD and 200 solvent molecules. The model exhibits good stereochemistry, with rmsd from ideality of 0.011 Å for bond lengths and 1.2° for bond angles (see Table 1). Pictures were generated with O,[35] GRASP,[37] MOLSCRIPT[38] and RASTER.[39]

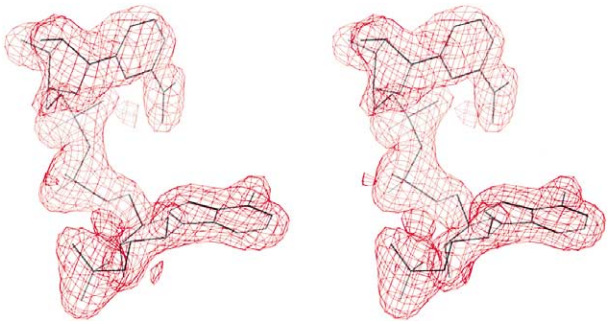

Figure 5. Stereoview of the electron density map for the complete $NADP^+$ molecule. The 2.1 Å resolution 2Fo−Fc map was calculated using phase information from the final model and contoured at 1.5 σ_{rms}.

Protein Data Bank accession numbers

The coordinates and structure factors for the FNR:$NADP^+$ complex have been deposited in the Protein Data Bank and were released with the date of publication (accession number 1GJR).

Acknowledgments

We are grateful to Dr J. K. Hurley and Professor G. Tollin (University of Arizona) and to Dr Martínez-Ripoll (CMBE, Madrid) for their collaboration in discussing different aspects of this work. This work was supported by grant BIO97-0912C02-01 from the CICYT to C.G.-M. and by grant P006/2000 from CONSID+DGA to M.M.

References

1. Karplus, P. A., Daniels, M. J. & Herriott, J. R. (1991). Atomic structure of ferredoxin–$NADP^+$ reductase: prototype for a structurally novel flavoenzyme family. *Science*, **251**, 60–66.
2. Bruns, C. M. & Karplus, P. A. (1995). Refined crystal structure of spinach ferredoxin reductase at 1.7 Å resolution: oxidized, reduced and 2′-phospho-5′-AMP bound states. *J. Mol. Biol.* **247**, 125–145.
3. Serre, L., Vellieux, F. M. D., Medina, M., Gómez-Moreno, C., Fontecilla-Camps, J. C. & Frey, M. (1996). X-ray structure of the ferredoxin:$NADP^+$ reductase from the cyanobacterium Anabaena PCC 7119 at 1.8 Å resolution, and crystallographic studies of $NADP^+$ binding at 2.25 Å resolution. *J. Mol. Biol.* **263**, 20–39.
4. Dorowski, A., Hofmann, A., Steegborn, C., Boicu, M. & Huber, R. (2001). Crystal structure of paprika ferredoxin–$NADP^+$ reductase. Implications for the electron transfer pathway. *J. Biol. Chem.* **276**, 9253–9263.
5. Correll, C. C., Ludwig, M. L., Bruns, C. M. & Karplus, P. A. (1993). Structural prototypes for an extended family of flavoprotein reductases: comparison of phthalate dioxygenase reductase with ferredoxin reductase and ferredoxin. *Protein Sci.* **2**, 2112–2133.
6. Correll, C. C., Batie, C. J., Ballou, D. P. & Ludwig, M. L. (1992). Phthalate dioxygenase reductase: a modular structure for electron transfer from pyridine nucleotide to [2Fe–2S]. *Science*, **258**, 1604–1610.
7. Lu, G., Campbell, W. H., Schneider, G. & Lindqvist, Y. (1994). Crystal structure of the FAD-containing fragment of corn nitrate reductase at 2.5 Å resolution: relationship to other flavoprotein reductases. *Structure*, **2**, 809–821.
8. Nishida, H., Inaka, K., Yamanaka, M., Kaida, S., Kobayashi, K. & Miki, K. (1995). Crystal structure of NADH-cytochrome b5 reductase from pig liver at 2.4 Å resolution. *Biochemistry*, **34**, 2763–2767.
9. Wang, M., Roberts, D. L., Paschke, R., Shea, T. M., Masters, B. S. & Kim, J. J. (1997). Three-dimensional structure of NADPH-cytochrome P450 reductase: prototype for FMN- and FAD-containing enzymes. *Proc. Natl Acad. Sci. USA*, **94**, 8411–8416.
10. Ingelman, M., Bianchi, V. & Eklund, H. (1997). The three-dimensional structure of flavodoxin reductase from *Escherichia coli* at 1.7 Å resolution. *J. Mol. Biol.* **268**, 147–157.
11. Gruez, A., Pignol, D., Zeghouf, M., Coves, J., Fontecave, M., Ferrer, J. L. & Fontecilla-Camps, J. C. (2000). Four crystal structures of the 60 kDa flavoprotein monomer of the sulfite reductase indicate a disordered flavodoxin-like module. *J. Mol. Biol.* **299**, 199–212.
12. Arakaki, A. K., Ceccarelli, E. A. & Carrillo, N. (1997). Plant-type ferredoxin–$NADP^+$ reductases: a basal structural framework and a multiplicity of functions. *FASEB J.* **11**, 133–140.
13. Batie, C. J. & Kamin, H. (1984). Electron transfer by ferredoxin:$NADP^+$ reductase. Rapid-reaction evidence for participation of a ternary complex. *J. Biol. Chem.* **259**, 11976–11985.
14. Karplus, P. A. & Schulz, G. E. (1989). Substrate binding and catalysis by glutathione reductase as derived from refined enzyme: substrate crystal structures at 2 Å resolution. *J. Mol. Biol.* **210**, 163–180.
15. Pai, E., Karplus, P. A. & Schulz, G. E. (1988). Crystallographic analysis of the binding of NADPH, NADPH fragments, and NADPH analogues to glutathione reductase. *Biochemistry*, **27**, 4465–4474.
16. Stehle, T., Claiborne, A. & Schulz, G. E. (1993). NADH binding site and catalysis of NADH peroxidase. *Eur. J. Biochem.* **211**, 221–226.
17. Li, R., Bianchet, M. A., Talalay, P. & Amzel, L. M. (1995). The three-dimensional structure of NAD(P)H: quinone reductase, a flavoprotein involved in cancer chemoprotection and chemotherapy: mechanism of the two-electron reduction. *Proc. Natl Acad. Sci. USA*, **92**, 8846–8850.
18. Chiu, H.-J., Johnson, E., Schröder, I. & Rees, D. (2001). Crystal structures of a novel ferric reductase from the hyperthermophilic archaeon *Archaeoglobus fulgidus* and its complex with $NADP^+$. *Structure*, **9**, 311–319.
19. Deng, Z., Aliverti, A., Zanetti, G., Arakaki, A. K., Ottado, J., Orellano, E. G. *et al.* (1999). A productive $NADP^+$ binding mode of ferredoxin–$NADP^+$ reductase revealed by protein engineering and crystallographic studies. *Nature Struct. Biol.* **6**, 847–853.
20. Mayoral, T., Medina, M., Sanz-Aparicio, J., Gómez-Moreno, C. & Hermoso, J. A. (2000). Structural basis of the catalytic role of Glu301 in *Anabaena* PCC 7119 ferredoxin–$NADP^+$ reductase revealed by X-ray crystallography. *Proteins: Struct. Funct. Genet.* **38**, 60–69.

21. Martinez-Julvez, M., Nogues, I., Faro, M., Hurley, J. K., Brodie, T. B., Mayoral, T. *et al.* (2001). Role of a cluster of hydrophobic residues near the FAD cofactor in *Anabaena* PCC 7119 ferredoxin–$NADP^+$ reductase for optimal complex formation and electron transfer to ferredoxin. *J. Biol. Chem.* **276**, 27498–27510.
22. Piubelli, L., Aliverti, A., Arakaki, A. K., Carrillo, N., Ceccarelli, E. A., Karplus, P. A. & Zanetti, G. (2000). Competition between C-terminal tyrosine and nicotinamide modulates pyridine nucleotide affinity and specificity in plant ferredoxin–NADP(+) reductase. *J. Biol. Chem.* **275**, 10472–10476.
23. Hunter, C. A. & Sanders, J. K. M. (1990). The nature of π–pi; interactions. *J. Am. Chem. Soc.* **112**, 5525–5534.
24. Sancho, J. & Gómez-Moreno, C. (1991). Interaction of ferredoxin–$NADP^+$ reductase from *Anabaena* with its substrates. *Arch. Biochem. Biophys.* **288**, 231–238.
25. Medina, M., Luquita, A., Tejero, J., Hermoso, J., Mayoral, T., Sanz-Aparicio, J. *et al.* (2001). Probing the determinants of coenzyme specificity in ferredoxin–$NADP^+$ reductase by site-directed mutagenesis. *J. Biol. Chem.* **276**, 11902–11912.
26. Medina, M., Martínez-Júlvez, M., Hurley, J. K., Tollin, G. & Gómez-Moreno, C. (1998). Involvement of glutamic acid 301 in the catalytic mechanism of ferredoxin–$NADP^+$ reductase from *Anabaena* PCC 7119. *Biochemistry*, **37**, 2715–2728.
27. Morales, R., Charon, M.-H., Kachalova, G., Serre, L., Medina, M., Gómez-Moreno, C. & Frey, M. (2000). A redox-dependent interaction between two electron-transfer partners involved in photosynthesis. *EMBO Rep.* **1**, 271–276.
28. Martínez-Júlvez, M., Hermoso, J., Hurley, J. K., Mayoral, T., Sanz-Aparicio, J., Tollin, G. *et al.* (1998). Role of Arg100 and Arg264 from *Anabaena* PCC 7119 ferredoxin–$NADP^+$ reductase for optimal $NADP^+$ binding and electron transfer. *Biochemistry*, **37**, 17680–17691.
29. Hurley, J. K., Cheng, H., Xia, B., Markley, J. L., Medina, M., Gómez-Moreno, C. & Tollin, G. (1993). An aromatic amino acid is required at position 65 in *Anabaena* ferredoxin for rapid electron transfer to ferredoxin–$NADP^+$ reductase. *J. Am. Chem. Soc.* **115**, 11698–11701.
30. Nishida, H., Inaka, K., Yamanaka, M., Kaida, S., Kobayashi, K. & Miki, K. (1995). Crystal structure of NADH-cytochrome b5 reductase from pig liver at 2.4 Å resolution. *Biochemistry*, **34**, 2763–2767.
31. Leslie, A. G. W. (1992). Molecular data processing. In *Crystallographic Computing 5: From Chemistry to Biology* (Moras, D., Podjarny, A. D. & Thierry, J. C., eds), pp. 39–50, Oxford University Press, Oxford, UK.
32. Collaborative Computational Project Number 4 (1994). The CCP4 suite: programs for protein crystallography. *Acta Crystallog. sect. D*, **50**, 760–763.
33. Navaza, J. (1994). AMoRe: an automated package for molecular replacement. *Acta Crystallog. sect. A*, **50**, 157–163.
34. Brünger, A. T. (1993). *X-PLOR: A System for X-ray Crystallography and NMR*, Yale University Press, New Haven, CT.
35. Jones, T. A., Zou, J. Y., Cowan, S. W. & Kjeldgaard, M. (1991). Improved methods for building protein models in electron density maps and the location of errors in these models. *Acta Crystallog. sect. A*, **47**, 110–119.
36. Brünger, A. T. (1992). The free *R* value: a novel statistical quantity for assessing the accuracy of crystal structures. *Nature*, **355**, 472–474.
37. Nicholls, A. & Honig, B. (1991). A rapid finite difference algorithm, utilizing successive over-relaxation to solve the Poisson–Boltzmann equation. *J. Comp. Chem.* **12**, 435–445.
38. Kraulis, P. J. (1991). MOLSCRIPT: a program to produce both detailed and schematic plots of protein structures. *J. Appl. Cryst.* **24**, 946–950.
39. Merritt, E. A. & Bacon, D. J. (1997). Raster3D: photorealistic molecular graphics. *Methods Enzymol.* **277**, 505–524.

Edited by R. Huber

(Received 22 January 2002; received in revised form 3 April 2002; accepted 12 April 2002)